European Food Research and Technology (2025) 251:1917–1933
https://doi.org/10.1007/s00217-025-04749-3

ORIGINAL PAPER

Layer-by-layer chitosan-based films with middle-layer incorporated rosemary oil nanoemulsion for sustained release and minced beef preservation

Neslihan Mutlu[1] · **Baycan Mor**[2]

Received: 17 February 2025 / Revised: 8 April 2025 / Accepted: 13 April 2025 / Published online: 29 April 2025
© The Author(s) 2025

Abstract
The aim of this study is to develop three-layer chitosan films enriched with rosemary oil nanoemulsion (RONE) at concentrations of 0.5%, 1%, and 1.5%, to to enhance antimicrobial properties and control oil release. Gas chromatography–mass spectrometry (GC–MS) identified 1,8-Cineole (20.52%), borneol (19.6%), and α-pinene (17.57%) as the main components of rosemary essential oil (REO). RONE prepared via ultrasonic homogenization, had a particle size of 70.75 nm, a polydispersity index (PDI) of 0.299, and a zeta potential of − 8 mV. Films with RONE exhibited reduced hydrophobicity and water vapor permeability (WVP) but maintained tensile strength (TS) and elongation at break (EAB). Scanning electron microscopy (SEM) confirmed smooth and compact film structures. Films containing 1% and 1.5% RONE showed enhanced antimicrobial activity against *Staphylococcus aureus* and *Bacillus subtilis*. Minced beef stored at 4 °C for 12 days with these films demonstrated reduced growth of *Pseudomonas* spp. and H_2S-producing bacteria. Additionally, peroxide value (PV) and total volatile nitrogen (TVN) levels remained within acceptable limits. These results highlight the potential of RONE-enriched chitosan-based multilayer films as sustainable food packaging solutions with antimicrobial, antioxidant, and prolonged-release properties to extend shelf life.

Keywords Multilayer film · Three-layer film · Rosemary essential oil · Minced beef · Chitosan · Nanoemulsion · Antimicrobial packaging

Introduction

Microbial contamination of food is an important public health issue as it leads to foodborne illnesses and food waste. Pathogenic microorganisms can contaminate food through various routes, such as raw materials, poor hygiene practices of food handlers, and inadequate cleaning of surfaces that come into contact with food [1, 2]. The World Health Organization has highlighted the significance of this issue by reporting that foodborne microbial contamination causes approximately 600 million illnesses and 420,000 deaths annually [3]. Additionally, microbial spoilage of food leads to 1.3 billion tons of food waste annually, resulting in a financial loss of 750 billion USD [4, 5]. Antimicrobial packaging emerges as a significant alternative to counter these risks. The incorporation of antimicrobial agents into food packaging materials can inhibit the growth of pathogenic microorganisms, preventing spoilage and extending the shelf life of food products while ensuring their safety [6, 7].

In recent years, numerous studies have focused on innovative strategies to improve food packaging systems, especially to address the challenges of microbial contamination, food spoilage, and quality deterioration during storage. Among these strategies, the incorporation of inorganic nanoparticles—such as nano-silver, nano-gold, zinc oxide nanoparticles (ZnO-NPs), and nano-titanium dioxide—has attracted considerable attention due to their high stability, broad-spectrum antibacterial activity, and compatibility with food packaging materials. In particular, ZnO-NPs have emerged as a promising candidate thanks to their

✉ Neslihan Mutlu
n.mutlu@kafkas.edu.tr

[1] Department of Biology, Faculty of Science and Letters, Kafkas University, Kars 36100, Turkey

[2] Department of Molecular Biology and Genetics, Faculty of Science and Letters, Kafkas University, Kars, Turkey

transparency, biocompatibility, and photocatalytic properties, and their use has been extensively studied in both intelligent and antimicrobial packaging applications [8]. In addition to antimicrobial and barrier functionalities, recent innovations in food packaging have also embraced the concept of intelligent packaging, which integrates sensing capabilities to monitor freshness and quality throughout the supply chain. However, challenges such as non-biodegradability and potential chemical migration have prompted a shift towards nature-inspired, biomimetic materials. These emerging materials, modeled after biological structures like plant cuticles, insect wings, and shell layers, offer promising solutions for extending food shelf life through mechanisms such as regulating respiration, inhibiting microbial growth, and enhancing moisture resistance—while aligning with principles of sustainability and safety [9]. Another innovative approach in food packaging involves the development of self-healing films and coatings. These materials can autonomously repair physical damage, thereby maintaining packaging integrity and helping preserve food quality for longer periods [10]. In parallel with the development of advanced packaging materials, there has been growing interest in incorporating natural bioactive agents into packaging systems. Among these, essential oils derived from plants have gained attention due to their recognized safety, broad-spectrum antimicrobial activity, and approval by regulatory agencies such as the FDA for food preservation purposes [11]. Essential oils (EOs) are natural antimicrobial agents capable of disrupting microbial cell structures and metabolic pathways, offering effective protection against a wide range of foodborne pathogens. Their antimicrobial efficacy can be significantly enhanced through synergistic combinations, allowing lower concentrations to be used without compromising effectiveness [12]. Compounds like eugenol and citral have demonstrated potent antimicrobial activity by increasing membrane permeability, promoting reactive oxygen species (ROS) generation, and impairing cellular integrity [13]. These properties support their growing application in food preservation, particularly in line with consumer demand for green, safe, and sustainable solutions. In addition to their antimicrobial effects, EOs are gaining attention for their potential to combat biofilms—highly structured microbial communities that form on food processing surfaces and pose significant risks to food safety. Biofilm formation progresses through initial microbial adhesion, extracellular polymeric substance production, and eventual maturation into a resilient three-dimensional matrix, from which bacteria can detach and spread [14]. Controlling biofilm-associated contamination is therefore critical in ensuring food hygiene. Despite their advantages, EOs also present technological challenges such as volatility, low water solubility, and instability under environmental stress. To overcome these limitations, encapsulation strategies such as nanoemulsions and edible coatings have been developed. These delivery systems help maintain EO activity, enhance dispersion in hydrophilic food environments, and protect sensory properties of food products. Among these, EO-incorporated edible coatings offer a particularly promising and eco-friendly solution, combining biodegradability with the ability to act as carriers for antimicrobial agents, antioxidants, or other bioactive compounds [15].

To enhance its stability and efficacy, REO can be formulated into nanoemulsions, which offer advantages such as improved physical stability and greater antimicrobial efficiency due to their small droplet size (< 200 nm) [16]. However, the rapid release of volatile components from films may limit long-term effectiveness [17, 18]. Multilayer film systems provide a solution by enabling sustained release and prolonged antimicrobial activity [19, 20]. Among biopolymers, chitosan stands out for its natural antimicrobial activity, biodegradability, and ability to improve film properties [21–26].

This study presents a novel approach to improving food packaging by developing three-layer chitosan-based films incorporated with RONE at concentrations of 0.5%, 1%, and 1.5% in the middle layer. While previous studies have mostly focused on monolayer films [27], this study explores a multilayer structure as a potential strategy for achieving more controlled release and prolonged antimicrobial activity. The films were characterized for their mechanical, barrier, optical, and structural properties, and their effectiveness was tested by packaging minced beef stored at 4 °C for 12 days. Compared to single-layer films, RONE-free multilayer films, and commercial plastic bags (CPB), the developed films showed promising results in reducing microbial growth and oxidative spoilage without compromising mechanical integrity. These findings suggest that RONE-loaded multilayer chitosan films may offer a biodegradable and efficient alternative for active food packaging.

Materials and methods

Materials

Chitosan (medium molecular weight), Tween 80, liquid glycerol, and magnesium oxide (97%) were obtained from Sigma Aldrich Chemie Gmbh (Darmstadt, Germany). REO was purchased from Arifoğlu Co. (Istanbul, Turkey). Plate count agar, Violet red bile agar, MRS-agar, and Pseudomonas selective agar were obtained from Merck (Darmstadt, Germany). Triple sugar iron agar was obtained from Neogen (Michigan, USA). Boric acid and potassium iodide were provided by Tekkim (Bursa, Türkiye). The bacteria strains

(*Escherichia coli* ATCC 35218, *Klebsiella pneumoniae* ATCC 700603, *Pseudomonas aeruginosa* ATCC 27853, *S. aureus* ATCC 29213, *B. subtilis* ATCC 6051) were obtained from the Laboratory of Microbiology, Biology Department, Kafkas University (Türkiye). All chemical reagents and materials used in this study were of analytical grade.

GC–MS

The chemical composition of REO was analyzed using a modified method based on Gao et al. [11], with an Agilent 7890B GC system coupled to a 5977B mass spectrometer (Agilent Technologies, USA), equipped with an HP-5MS UI capillary column (30 m × 0.25 mm i.d., 0.25 µm film thickness). Prior to injection, REO was diluted 1:100 (v/v) in *n*-hexane (HPLC grade), and 1 µL of the diluted solution was injected in splitless mode. The injector temperature was maintained at 250 °C. The oven temperature program was: initial 60 °C (held 3 min), ramped at 3 °C/min to 250 °C, and held at 250 °C for 5 min. Helium was used as the carrier gas at a constant flow rate of 1.0 mL/min. The mass spectrometer was operated in electron impact (EI) mode at 70 eV with a source temperature of 230 °C. Mass spectra were recorded over a scan range of 40–500 *m/z*. Each sample was analyzed in duplicate. Compound identification was performed by comparing the mass spectra with those in the NIST 2017 library database (similarity index ≥90%).

Preparation and characterization of rosemary nanoemulsion

To prepare RONE containing 10% REO, REO at a concentration of 10% (v/v) and Tween 80 at 30% (v/v) of the REO were gradually added to distilled water at room temperature using a magnetic stirrer at 300 rpm. To convert this coarse emulsion into nanoemulsion, an ultrasonic homogenizer (Ultrasonic homogenizer HD 3200 Bandelin Sonopuls, Berlin, Germany) was employed. The homogenizer probe (MS 72) was immersed 10 mm below the emulsion surface and operated at 40% amplitude for 10 min. To prevent the temperature of the emulsion from exceeding 30 °C, the sample was placed in ice. The prepared NE was stored in a dark glass container at 4 °C. The particle size, PDI, and zeta potential of the prepared emulsion were determined using an analysis instrument (Malvern Zetasizer Nano ZSP, Worcestershire, UK). Before experiments, the NE was diluted (1:50) with distilled water. The mean droplet size of RONE was measured with dynamic light scattering (DLS) at 25 °C and 633 nm [28]. Each determination was run in triplicate.

Preparation of chitosan solution

Chitosan solution at a concentration of 1.5% was prepared in a 1% glacial acetic acid. Glycerol was added as a plasticizer (30% (wt/wt) on solid content) to the mixture. To ensure complete dissolution of chitosan in the mixture, it was stirred at 300 rpm at room temperature for approximately 12 h. This solution was used for the bottom and top layers. To prepare the inner layer of the films, nanoemulsion, chitosan solution, and distilled water were mixed at appropriate amounts to achieve final concentrations of 0.5%, 1%, and 1.5% RONE and 1% chitosan, stirred at 300 rpm for 10 min.

Preparation of three-layer films

The chitosan layer containing RONE was sandwiched between two chitosan layers, and all drying processes were carried out at room temperature. For this, approximately 10 g of chitosan solution was poured into petri dishes (9 cm) and after about 10 h, when it had a dry but adhesive surface, about 10 g of the chitosan layer containing RONE was poured on top. The inner layer was allowed to dry for about 6 h, and then another chitosan layer of 10 g was poured, and the films were allowed to dry completely. The films removed from the petri dishes were used for analysis, while those poured onto 23 cm Teflon plates were used for food packaging. Groups containing 1.5%, 1%, and 0.5% RONE were named as CH +1.5% RONE, CH +1% RONE, and CH +0.5% RONE, respectively. A control group (CH), consisting of films with only chitosan layers, without the RONE-containing layer, was also prepared. A monolayer film containing 1.5% RONE (CH +1.5% RONE (m)) was prepared to compare whether the oil release occurs in a controlled manner. In addition to the prepared films, food packaging was also done with a CPB to compare chemical and microbiological changes. CH +1.5% RONE (m) and CPB have only been used in food packaging.

Microstructure of films

The microstructural properties of the films were investigated using SEM (Carl Zeiss Gemini 300, Germany). Prior to examination, film samples were gold-coated under vacuum, placed on a holder, and photographed at low voltage of 15 kV, both in surface and cross-sectional areas [28].

Mechanical properties of films

The thickness of the films was measured at five randomly selected locations using a digital micrometer (Loyka 5203, Ankara, Turkey). TS and EAB (%) values were determined using a tensile testing machine (Testform/AS1, Ankara,

Turkey). The film samples were cut into strips (6 cm × 1 cm) and tested. Initial grip separation was 40 mm/min, and crosshead speed was 50 mm/min. Measurements were performed in triplicate [28].

Contact angle

The hydrophobic/hydrophilic properties of the films were determined by contact angle measurements. Approximately 5 µL of ultra-pure water droplets were carefully deposited onto the film surface (2 cm × 2 cm) using a micro-syringe. The angle on each side of the droplet was measured and photographed at room temperature. Results are expressed as the average of three measurements.

Color and whiteness index

The CIELab color coordinates of the films (L* (lightness), a* (red-green), and b* (yellow-blue)) were determined using a color spectrophotometer (X-Rite Ci7800, Michigan, USA) [28]. With these results, the films' total color change (ΔE) and whiteness index (WI) were calculated using the following Eqs. (1) and (2):

$$\Delta E = \sqrt{(L^* - L_s^*)^2 + (a^* - a_s^*)^2 + (b^* - b_s^*)^2}. \quad (1)$$

$$WI = 100 - \sqrt{(100 - L^*)^2 + (a^*)^2 + (b^*)^2}. \quad (2)$$

where L_s* (95.69), a_s* (−0.37), and b_s* (2.14) are the measurement results of a standard blank plate, and L*, a*, and b* are the values corresponding to the samples. The measurements were run in triplicate.

Water vapor permeability, moisture content, and water solubility

To determine the WVP values of films, the ASTM E96 method was used [29].

To determine the moisture content (MC) of films, samples of each film (2 cm x 2 cm) were cut and weighed, then dried in an oven at 105 ±1 °C until reaching a constant weight. MC was determined using the Eq. (3):

$$MC\ (\%) = \frac{m_1 - m_2}{m_1} \times\ 100, \quad (3)$$

where m_1 and m_2 are the initial and the dried sample weight, respectively.

To assess water solubility (WS) of the films, small pieces of the films (3 cm × 3 cm) were prepared, weighed, and subjected to drying in an oven at 105 °C for 24 h. These film samples were then immersed in 50 mL of distilled water at room temperature for 24 h with gentle stirring. Subsequently, the remaining film residues were re-dried in the oven at 105 °C until reaching a constant weight. The solubility (%) of the film samples was calculated using the following Eq. (4):

$$WS\ (\%) = \frac{Initial\ dried\ mass\ of\ film - final\ dried\ mass\ of\ film}{Initial\ dried\ mass\ of\ film} \times 100 \quad (4)$$

The experiments were run in triplicate.

In vitro antibacterial properties of the films

The in vitro antimicrobial properties of the films were determined using the disk diffusion method. Three Gram-negative strains (*E. coli*, *K. pneumoniae*, *and P. aeruginosa*) and two Gram-positive strains (*S. aureus*, *B. subtilis*) were used. The strains were inoculated onto Mueller-Hinton agar and incubated at 37 °C for 12 h, then suspended in sterile saline solution and adjusted to a 0.5 McFarland standard (1.5×10^8 CFU/mL). This bacterial suspension was evenly spread onto Mueller-Hinton agar plates using sterile swabs. Circular films, with a diameter of 6 mm, were sterilized under ultraviolet light for 30 min and subsequently placed on the agar. The plates were then incubated at 37 °C for 24 h. The diameter of the resulting inhibition zones (mm) was measured. The experiments were run in triplicate.

Sample preparation

Minced beef from the same batch was purchased from a local market in Kars, Turkey. The minced beef was weighed into 50 g portions and wrapped with the following film samples:

CPB.
CH.
CH + 0.5%RONE.
CH + 1%RONE.
CH + 1.5%RONE.
CH + 1.5%RONE (m).

The films were covered entire surface of the minced beef samples and placed in sterile polyethylene bags. CPB, CH, and CH + 1.5% RONE (m) films were used as controls. All samples were stored at 4 °C for 12 days. Microbiological and chemical analyses were conducted three-day intervals.

Chemical analyses

Lipid oxidation was determined using 2-thiobarbituric reactive substances (TBARS) assay as reported by Setyabrata

and Kim [30]. Five grams of the sample were homogenized with 15 mL of distilled water and 50 µL of 10% butylated hydroxyanisole. Subsequently, 1 mL of the homogenate was mixed with 2 mL of a 20 mM solution of 2-thiobarbituric acid in 15% trichloroacetic acid. The mixture was then heated for 15 min in an 80 °C water bath and cooled for 10 min in an ice water bath. After centrifugation at 2000*g* for 10 min, the supernatant was filtered through filter paper. The absorbance was measured at 531 nm, and the TBARS value was expressed as mg malondialdehyde (MDA)/kg meat.

To determine the PV, the minced beef sample (5 g) was mixed with 30 ml of glacial acetic acid: chloroform (3:2, v/v) and 0.5 ml of saturated potassium iodide, and kept in dark conditions for 2 min. Then, 30 ml of distilled water and 1 mL of starch solution (1%, w/v) were added, and the sample was shaken for 3–6 s at 25 ± 1 °C. Titration was carried out using 0.01 N sodium thiosulfate and the result was expressed as mEq peroxide/1000 g lipid [31].

TVN was measured following Mohammadi et al.'s [32]. protocol. Briefly, minced beef (10 g) was mixed with 100 mL distilled water, homogenized, shaken, and then centrifuged at 3000 rpm for 10 min. The filtered supernatant (5 mL) was alkalized with MgO solution (5 mL, 10 g/L). Steam distillation for 5 min using a Kjeldahl distillation unit yielded a distillate collected in a flask containing boric acid solution and indicators. The distillate solution titrated with 0.1 mol/L HCl and TVN content expressed as mg N/100 g meat.

Table 1 Quantative composition (%) of rosemary essential oil

No.	Retention Time	Composition %	Compound	Qual
1	5.24	0.16	α-Thujene	97
2	5.42	17.57	α-Pinene	86
3	5.80	4.68	Camphene	96
4	6.44	1.12	Sabinene	96
5	6.55	2.35	β-Pinene	95
6	6.90	0.40	β-Myrcene	96
7	7.52	0.48	(+)−3-Carene	96
8	7.72	0.25	α-Terpinene	98
9	7.97	6.45	p-Cymene	97
10	8.11	8.07	D-Limonene	99
11	8.20	20.52	1,8-Cineole	97
12	9.13	1.16	γ-Terpinene	97
13	10.20	0.31	Menthene	97
14	10.61	1.92	Linalool	96
15	12.35	2.49	Camphor	98
16	12.85	19.60	Borneol	91
17	13.68	0.63	Terpinen-4-ol	94
18	14.22	5.97	α-Terpinyl	90
19	14.50	0.77	Dihydro-β-terpineol	95
20	18.25	3.24	Isobornyl acetate	96
21	23.70	1.10	Caryophyllene	99
Total		99.24		

Microbiological analyses

The packaged minced beef samples were microbiologically evaluated over a period of approximately two weeks at 3-day intervals. Approximately 10 g of minced beef was placed in stomacher bags containing 90 mL of 0.1% peptone and homogenized for 5 min. Subsequently, appropriate serial decimal dilutions of the samples were prepared, and 100 µL of each dilution was inoculated onto agar plates and spread plated. Plate count agar (Merck, Darmstadt, Germany) was used for total viable counts (TVC), Man Rogosa Sharpe agar (Merck, Darmstadt, Germany) for lactic acid bacteria (LAB), violet red bile glucose agar (Merck, Darmstadt, Germany) for *Enterobacteriaceae*, Pseudomonas-selective agar (Merck, Darmstadt, Germany) for *Pseudomonas* spp., and Iron agar (Neogen, MI, USA) for H_2S-producing bacteria. Bacterial counts were expressed as log colony-forming units per gram (CFU/g).

Statistical analysis

Differences between the results were determined by One-way ANOVA and Tukey tests using SPSS version 22 (Chicago, IL, USA), with differences between mean values considered significant at a 5% level of significance.

Results and discussion

Chemical composition of rosemary essential oil

The chemical composition of REO has been extensively researched. It has been observed that the essential oil of *S. rosmarinus* contains various components, and these vary depending on factors such as the plant's genetic differences and geographical origin. Techniques such as GC, MS, and nuclear magnetic resonance have been used in studies to analyze the chemical composition of the plant's essential oil [33, 34]. Among the main chemical components identified in the essential oil of *S. rosmarinus* are eucalyptol (1,8-Cineole), verbenone, bornyl acetate, alkaloids, flavonoids, phenols, rosmarinic acid, mineral components, vitamin A, and vitamin C [35, 36]. In this study, a composition like the previously identified ROEO oil contents was detected. Chemical analysis revealed the presence of 21 compounds (Table 1; Fig. 1), including 1,8-Cineole (20.52%), borneol (19.6%), and α-pinene (17.57%) as major compounds. It has been found that the ROEO exhibits antimicrobial, antifungal, antioxidant, and antiproliferative activities, indicating its potential for various medical and industrial applications [37].

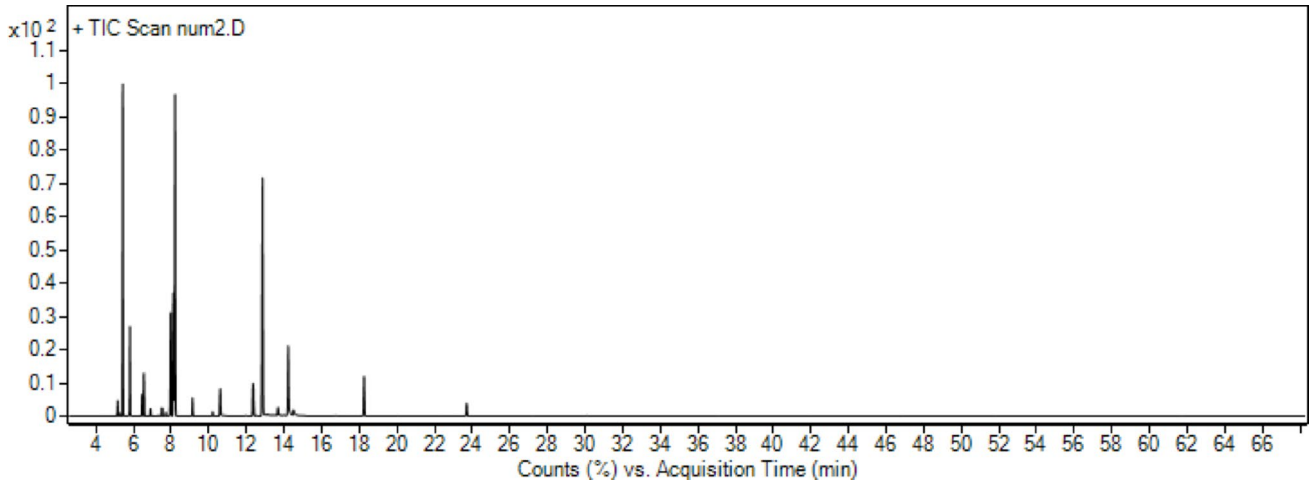


Fig. 1 GC–MS chromatogram of rosemary essential oil

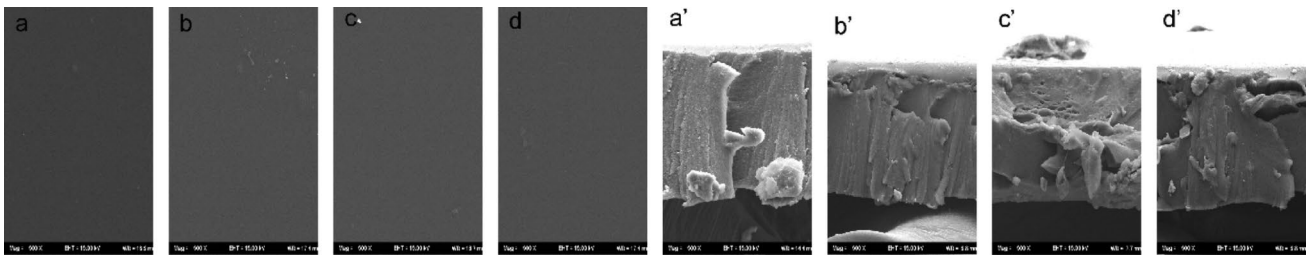


Fig. 2 SEM images of surface (**a**–**d**) and cross-section (**a′**–**a′**) of the control film and films containing 0.5%, 1% and 1.5% of RONE, respectively

Nanoemulsion characterization

The particle size, PDI value, and zeta potential of the prepared NE were determined to be 70.75 ± 1.813 nm, 0.299 ± 0.019, and −8 ± 0.494 mV, respectively. The particle size, PDI value, and zeta potential of nanoparticles are crucial factors that determine their characteristics and behavior.

A PDI of 0.299 ± 0.019 indicates a relatively uniform particle size distribution, which ensures consistent nanoparticle properties and performance [38]. Particle size significantly impacts various nanoparticle properties, as emphasized by Hanasaki et al. [39]. The observed particle size of 70.75 ± 1.813 nm, within the nanoscale range, is advantageous due to its high surface area-to-volume ratio and potential quantum effects. Woehl et al. [40] discuss nanoparticle growth kinetics and size distribution, highlighting insights into growth mechanisms and stability.

Zeta potential influences colloidal stability and interactions of nanoparticles [41]. A zeta potential of − 8± 0.494 mV suggests moderate colloidal stability, as values near zero indicate limited repulsive forces, while the negative surface charge enhances dispersion stability and prevents aggregation.

Preparation parameters, such as polymer concentration and stirring time, significantly influence nanoparticle size and zeta potential [42]. Additionally, pH plays a critical role in modulating zeta potential, affecting stability and particle interactions in different environments [43].

In summary, the obtained values (70.75 ± 1.813 nm, 0.299 ± 0.019, and −8 ± 0.494 mV) confirm the nanoparticles' nanoscale size, uniform size distribution, and negative surface charge. These characteristics significantly influence their stability, interactions, and potential applications.

Microstructure of films

Several studies have demonstrated that oil nanoemulsions can cause the formation of pores and a rough structure on the film surface [28, 44, 45], whereas in our examination of the microstructural properties of the films, no pore structure is seen in the surface images, and a compact structure is observed (Fig. 2). This suggests that the essential oil did not rise to the surface during the preparation and drying stages of the films. It is observed that the substances used cause a small amount of aggregation due to the zeta potential. Additionally, in the cross-sectional photos, it is seen that the porous structure caused by the oil droplets remains below the surface.

Table 2 Mechanical properties of films

Sample	Thickness (mm)	TS (MPa)	EAB (%)
CH	0.68 ± 0.09[a]	2.99 ± 1.15[a]	77.52 ± 14.91[a]
CH + 0.5%RONE	0.89 ± 0.02[a]	3.29 ± 0.61[a]	65.78 ± 5.33[a]
CH + 1%RONE	0.90 ± 0.01[a]	3.11 ± 0.80[a]	73. 03 ± 6.91[a]
CH + 1.5%RONE	0.89 ± 0.01[a]	2.91 ± 0.67[a]	70.91 ± 3.66[a]

Data are mean ± SD. Different letters in the same column indicate significant differences ($p < 0.05$)

Mechanical properties of films

As shown in Table 2, incorporating oil nanoemulsion into the film matrix did not cause a statistically significant difference in TS and EAB ($p > 0.05$). This can be attributed to the effective formation of the nanoemulsion. The stability and homogeneous distribution of the nanoemulsions within the film matrix play a critical role in maintaining the mechanical properties of the film. When the oil is successfully incorporated into the nanoemulsion system, it can be homogeneously distributed within the film matrix without causing aggregation or phase separation. This homogeneous distribution ensures that the mechanical properties of the film, such as TS and EAB, remain unaffected [46].

Additionally, the use of appropriate emulsifiers or stabilizers in the nanoemulsion formulation can contribute to the preservation of the film's integrity. These emulsifiers help form a stable interfacial layer around the oil droplets, preventing aggregation and ensuring their homogeneous distribution within the film matrix. As a result, the mechanical properties of the film are maintained, and no changes may be observed in the TS and EAB values [47].

Hydrophobicity of films

The contact angle is an important parameter in characterizing the wettability properties of the produced materials. The decrease in the hydrophobicity of the materials, resulting in increased wettability, can create a suitable humid environment for microorganisms.

Although there was no change in TS and EAB values, a decrease in hydrophobicity of films containing RONE was observed (Fig. 3). Despite the surface of the films coated with the same material, the contact angles of the films varied. These factors may collectively contribute to the observed differences in contact angles, including the migration of the oil from its initial region during the preparation and drying, changes in surface roughness due to varying nanoemulsion concentrations, the chemical composition of the nanoemulsion (particularly essential oils and surfactants), differences in film thickness and density affecting water interaction, and variations in production process parameters such as temperature and pressure impacting the distribution and surface effects of the nanoemulsion [48, 49].

Color and whiteness index

The values for L*, a*, and b* determined by the color spectrometer, along with the ΔE and WI values calculated using the formulas provided in the methods section, are presented in Table 3 below. In films containing 1% or more RONE, lightness decreased, while in films containing 0.5% or more RONE, yellowness and total color change increased. Additionally, the WI decreased as the oil content increased ($p < 0.05$). Our findings align with those of Frank et al. [50] and

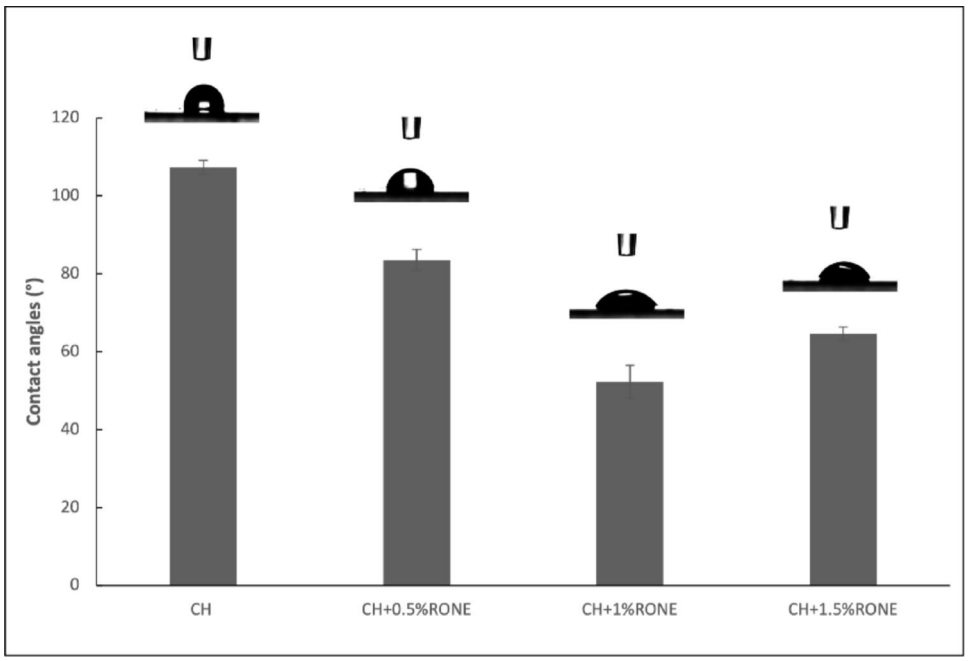


Fig. 3 Contact angles of films

Table 3 Color measurements of film

Data are mean ± SD. Different letters in the same column indicate significant differences ($p < 0.05$)

Sample	L*	a*	b*	ΔE	WI
CH	93.42 ± 0.28^{a}	− 1.48 ± 0.01^{a}	8.56 ± 0.29^{c}	6.90 ± 0.37^{c}	89.10 ± 0.40^{a}
CH + 0.5%RONE	93.04 ± 0.22^{a}	− 2.05 ± 0.25^{b}	11.65 ± 0.96^{b}	10.01 ± 0.95^{b}	86.37 ± 0.75^{b}
CH + 1%RONE	91.98 ± 0.36^{b}	− 2.25 ± 0.23^{b}	14.54 ± 1.29^{a}	13.07 ± 1.35^{a}	83.24 ± 1.30^{c}
CH + 1.5%RONE	92.31 ± 0.06^{b}	− 2.30 ± 0.24^{b}	14.53 ± 0.96^{a}	12.99 ± 0.94^{a}	83.39 ± 0.86^{c}

Table 4 WVP, MC (%), and WS of films

Sample	MC (%)	WVP (x 10^{-7} g.m/m^2. Pa.h)	WS (%)
CH	21.41 ± 1.18^{a}	4.93 ± 0.85^{a}	23.69 ± 1.89^{a}
CH + 0.5%RONE	19.94 ± 0.14^{a}	4.90 ± 0.10^{a}	23.48 ± 1.46^{a}
CH + 1%RONE	20.98 ± 1.73^{a}	4.91 ± 0.17^{b}	20.97 ± 1.05^{ab}
CH + 1.5%RONE	19.23 ± 1.57 ^{a}	4.77 ± 0.25^{b}	19.55 ± 0.34^{b}

Data are mean ± SD. Different letters in the same column indicate significant differences ($p < 0.05$)

Taqi et al. [51], demonstrating that the incorporation of oil nanoemulsions into biocomposite films results in significant changes in color properties. Specifically, we observed a decrease in lightness and WI, alongside an increase in yellowness and total ΔE ($p < 0.05$). These alterations can be attributed to light scattering caused by lipid droplets in the oil nanoemulsions, which reduces lightness and enhances yellowness. Consequently, the presence of oil components in the film matrix significantly impacts the overall appearance and color characteristics of the films.

Water vapor permeability, moisture content, and water solubility

As shown in Table 4, while the MC values of the films remained unchanged ($p > 0.05$), examination of the WVP and WS properties of the films reveals that these values decrease as the proportion of incorporated oil increases. Notably, the changes are statistically significant in films incorporated with 1% and 1.5% RONE ($p < 0.05$).

The decrease in WVP and WS in films incorporated with oil nanoemulsions can be attributed to several factors. Cerqueira et al. [52] highlighted that the reduction in WVP values in chitosan films with added oil could be explained by the decrease in the hydrophilic portion of the film, leading to a lower affinity for water molecules. This alteration in the film's composition affects its interaction with water vapor, resulting in reduced permeability. Similarly, Restrepo et al. [53] observed that essential oil nanoemulsions had a plasticizing effect on films, increasing WVP while the oils' hydrophobic nature contributed to decreased water solubility.

Furthermore, Yu et al. [44] found a negative correlation between film water solubility and the concentration of *Melissa officinalis*. Additionally, Souza et al. [54] also reported a decrease in WVP in chitosan films modified with lipid fractions, indicating the impact of lipid incorporation on film permeability.

In summary, the decrease in moisture content, WVP, and water solubility in films incorporated with oil nanoemulsions can be attributed to changes in film composition, hydrophilicity, and structure induced by the addition of hydrophobic materials. These alterations influence the film's interaction with water molecules, permeability characteristics, and overall solubility, highlighting the complex interplay between nanoemulsions and film properties.

In our study, despite the decrease in contact angle values, this reduction can be attributed to the nanoemulsion droplets not reaching the surface. The localized effects of the oil droplets, improved cross-linking, reduced free volume, and enhanced barrier properties collectively contribute to lower WVP and WS.

In vitro antibacterial properties of the films

As shown in Table 5, for *S. aureus* and *B. subtilis*, the inhibition zones increased as the concentration of RONE increased, with the highest antibacterial effect observed at 1.5% RONE ($p < 0.05$), suggesting a dose-dependent effect. A similar trend is observed for *P. aeruginosa*, *E. coli*, and *K. pneumoniae*, though the increments are more moderate. These findings suggest that the addition of RONE to CH films improves their antimicrobial efficacy, particularly at higher concentrations, against both Gram-positive and

Table 5 In vitro antimicrobial activity of films

Data are mean ± SD. Different letters in the same row indicate significant differences ($p < 0.05$)

Strains	Zone of inhibition (mm)			
	CH	CH + 0.5%RONE	CH + 1%RONE	CH + 1.5%RONE
S. aureus (ATCC 29213)	8.40 ± 0.36^{b}	9.13 ± 0.23^{b}	10.63 ± 0.32^{a}	11.10 ± 0.65^{a}
B. subtilis (ATCC 6051)	8.80 ± 0.26^{b}	8.83 ± 1.89^{b}	11.20 ± 0.50^{ab}	11.96 ± 0.45^{a}
P. aeruginosa (ATCC 27853)	6.60 ± 0.36^{b}	6.40 ± 0.52^{b}	7.5 ± 0.43^{ab}	8.06 ± 0.51^{a}
E. coli (ATCC 35218)	7.10 ± 0.30^{c}	7.33 ± 0.30^{bc}	7.96 ± 0.15^{ab}	8.20 ± 0.30^{a}
K. pneumoniae ATCC 700,603	7.90 ± 0.45^{b}	7.96 ± 0.64^{b}	8.63 ± 0.15^{ab}	8.10 ± 0.26^{a}

Gram-negative bacteria. These results align with existing literature, which attributes the improved antimicrobial efficacy of nanoemulsion-infused films to the small droplet size and increased bioavailability of the active compounds. For instance, Lu et al. [55] reported that the enhanced surface area of nanoemulsions facilitates stronger interactions with microbial cell membranes, leading to increased antibacterial effects. Similarly, Amjadi et al. [16] demonstrated that the incorporation of essential oil nanoemulsions into films improved the solubility and dispersion of the active compounds, resulting in enhanced antibacterial performance. The trend observed in this study, where higher concentrations of RONE resulted in greater antibacterial activity, supports the findings of Wang et al. [56], who noted that smaller droplets with higher surface area exhibit greater bactericidal effects. Additionally, the slow and sustained release of the active components in nanoemulsions, as described by Hassanzadeh et al. [57], likely contributed to the increased antimicrobial activity observed in the films with higher concentrations of RONE.

Chemical analyses

PV measures the amount of hydroperoxides formed during the early stages of lipid oxidation and indicates the oxidative quality and deterioration of fats [58, 59]. Monitoring PV is important to ensure that foods remain within acceptable quality standards throughout their shelf life, thereby protecting consumer health [60].

The World Health Organization (WHO) and the Food and Agriculture Organization (FAO) recommend a maximum PV of 10 mEq O_2/kg for edible oils [61].

When the PV results measured in our study were evaluated, it was observed that, as shown in Fig. 4a, there were no statistically significant differences in the values measured across all days between the CPB, CH, and CH + 0.5% RONE treated groups ($p > 0.05$). By the end of day 12, the PV values in all groups remained below the acceptable threshold. The slower increase in PV observed in the CH + 1.5% RONE treated group between days 8 and 12 suggests prolonged antioxidant activity. However, the PV values of the CH + 1.5% RONE and CH + 1.5% RONE(m) treated groups on day 12 were statistically similar ($p > 0.05$), likely due to the antioxidant capacity reaching saturation, resulting in comparable levels of lipid oxidation.

TBARS is an indicator of malondialdehyde (MDA), a secondary product formed during the oxidative degradation of polyunsaturated fatty acids. The TBARS assay is significant because it provides insights into the freshness and quality of food, as lipid oxidation can lead to rancidity, off-flavors, and a reduction in nutritional value [62].

Acceptable limits for TBARS values for fresh products should ideally be below 3 mg MDA/kg [63, 64]. As seen in Fig. 4b, on day 4, the values in all groups were measured to be within acceptable limits. However, the TBARS values were found to be lower in the other groups compared to the CPB treated group ($p < 0.05$). By day 8, the values obtained were found to be within acceptable limits in the CH + 1% RONE, CH + 1.5% RONE, and CH + 1.5% RONE (m) treated groups. On day 12, the highest TBARS values (4.81 mg MDA/kg) were recorded in the CPB group, while the lowest values were found in the CH + 1% RONE, CH + 1.5% RONE, and CH + 1.5% RONE (m) treated groups, with the values in the CH + 1.5% RONE and CH + 1.5% RONE (m) treated groups remaining within acceptable limits. Notably, the TBARS levels in the CH + 1.5% RONE group showed a decrease between days 8 and 12, which could be attributed to prolonged antioxidant activity. Similar to our study, studies have shown a positive correlation between PV and TBARS values, particularly in the context of lipid oxidation in food products. For example, research indicates that an increase in PV often corresponds with an increase in TBARS, suggesting that as lipids oxidize, both primary and secondary products accumulate [65]. However, the relationship may not always be linear, as certain conditions can lead to discrepancies between the two measurements [66].

Chitosan possesses significant antioxidant properties primarily due to its free radical scavenging ability. Chitosan derivatives have been found to be more effective in scavenging carbon-centered radicals compared to unmodified chitosan. Moreover, it has been demonstrated that the antioxidant activity of chitosan is enhanced when combined with substances such as essential oils. Research by Yu et al. [67] demonstrated that chitosan coatings combined with essential oils significantly improved the antioxidant properties of grass carp fillets stored at + 4 °C. The study found that the presence of chitosan and essential oils effectively reduced lipid oxidation, suggesting enhanced antioxidant activity.

The combination of chitosan and REO has been demonstrated to significantly enhance antioxidant properties. REO is a potent source of bioactive compounds, including carnosic acid, rosmarinic acid, and various polyphenols, which collectively contribute to its remarkable antioxidant activity [68, 69].

Measuring TVN values can guide consumers, especially in determining the freshness of fish and meat products. As microorganisms proliferate, they produce volatile nitrogenous compounds, causing an increase in TVN levels [70]. For example, TVN values of 15–20 mg N/100 g in fish indicate good quality, while values exceeding 35 mg N/100 g suggest spoilage [71].

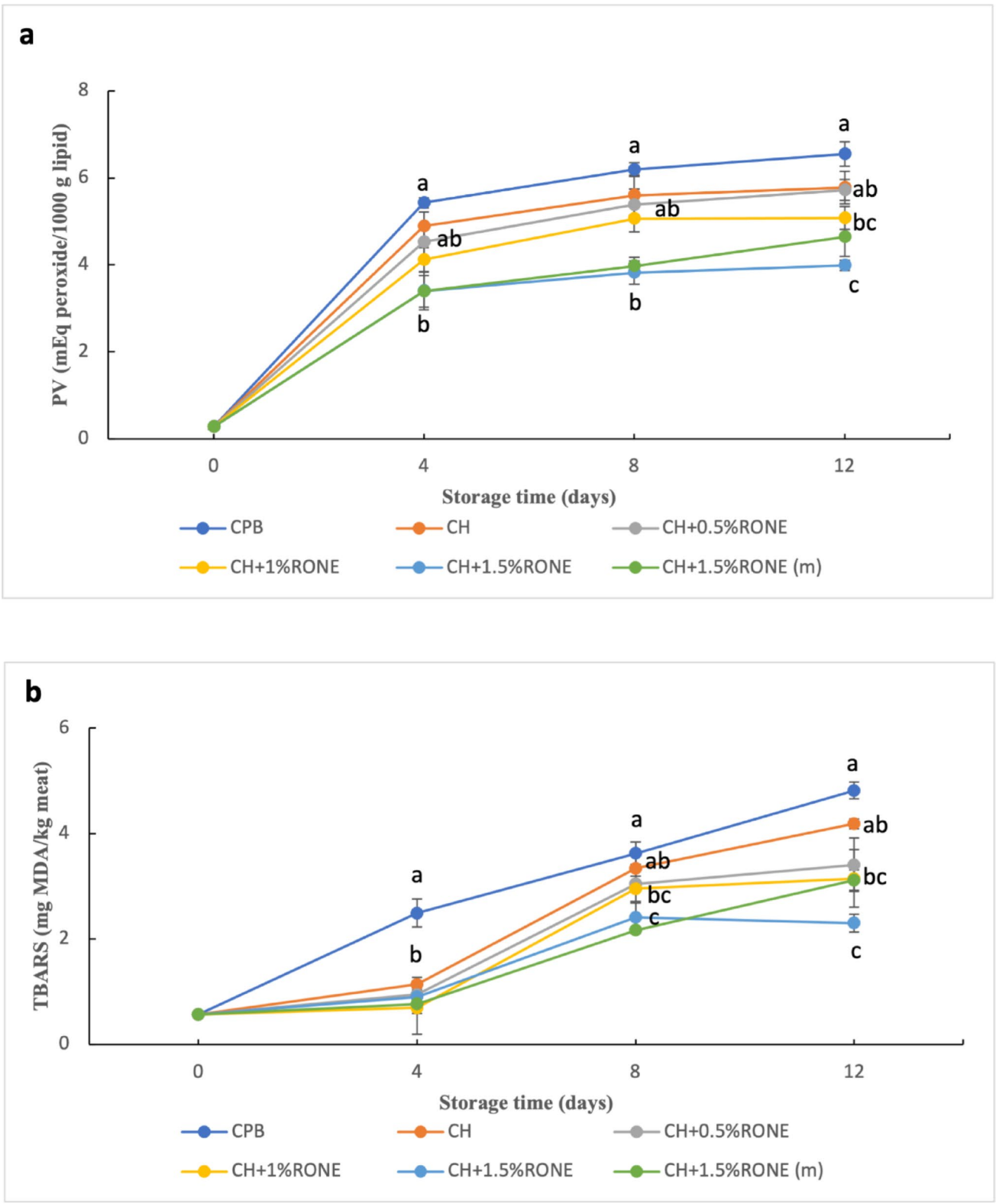


Fig. 4 Changes in PV (**a**), TBARS (**b**), and TVN (**c**) values of minced beef during storage

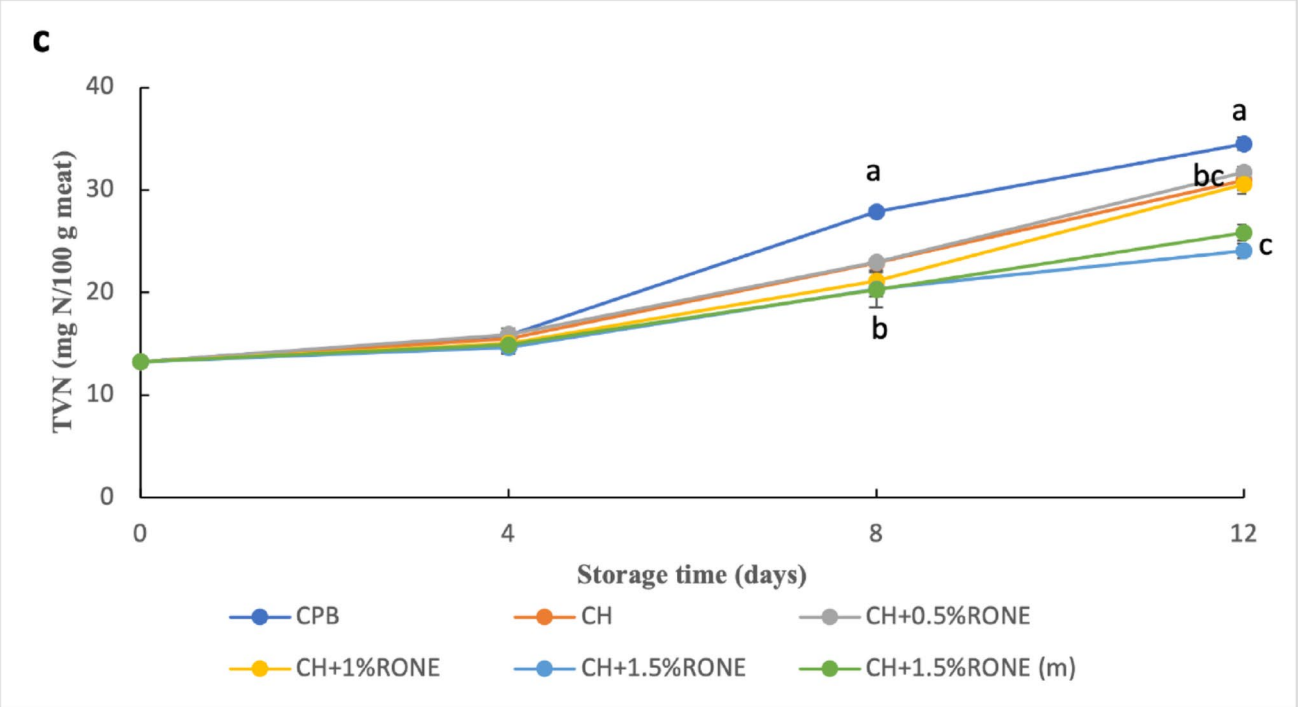


Fig. 4 (continued)

There were no significant differences between the groups on day 4 ($p > 0.05$). However, on day 8, the TVN value of the sample covered with a CPB was significantly higher than those of the other groups ($p < 0.05$). This difference is likely due to the antimicrobial properties of the CH-containing films.

On day 12, the TVN value in the CPB treated group was found to exceed 34,49 mg N/100 g and was significantly higher compared to the other groups ($p < 0.05$). The lowest TVN values (24.07 mg N/100 g) were measured in the CH + 1.5% RONE group. On day 12, although there was no statistically significant difference between the CH + 1.5% RONE and CH + 1.5% RONE (m) treated groups ($p > 0.05$), the lower increase in TVN values observed in the CH + 1.5% RONE treated group could be attributed to the extended antimicrobial activity, which may have contributed to better preservation of protein quality over time.

Chitosan's polycationic nature enables it to disrupt bacterial membranes, exhibiting antibacterial activity against pathogens such as *E. coli*, *S. aureus*, and *K. pneumoniae* [72, 73]. The synergistic effect of chitosan and REO is attributed to the rich chemical composition of REO, which includes compounds like carnosic acid and α-pinene that disrupt bacterial membranes and inhibit protein synthesis [9, 74]. As reported by Farokhzad et al. [75] and Abdollahi et al. [27], the incorporation of REO, which exhibits strong antimicrobial activity, further enhances the preservation of food quality by lowering TVN levels during storage, aligning with the results observed in this study.

Microbiological analyses

The microbial counts in the packaged foods are shown in Fig. 5. There were no differences in the initial microbial loads among the groups. However, the total TVC on days 4, 8, and 12 was significantly higher in samples covered with CPB compared to the other groups ($p < 0.05$). On day 12, the CPB and CH treated groups exceeded the recommended TVC limit of 7 log CFU/g, whereas the other treated groups remained below this threshold, indicating that RONE enhanced antimicrobial activity.

The difference between the CH + 1.5% RONE and CH + 1.5% RONE (m) treated groups became evident on day 12. While both groups demonstrated similar antimicrobial effects on earlier days, the TVC increase on day 12 was lower in the CH + 1.5% RONE treated group compared to the monolayer film treated group. This result could be attributed to the controlled release of RONE, resulting in prolonged antimicrobial activity.

It can be concluded that the films containing RONE extended the storage time up to 12 days. Similarly, The release of vanillin from polyvinyl alcohol and bacterial cellulose films was studied, showing that multilayer films, consisting of external bacterial cellulose layers and an inner vanillin-containing layer, resulted in slower release

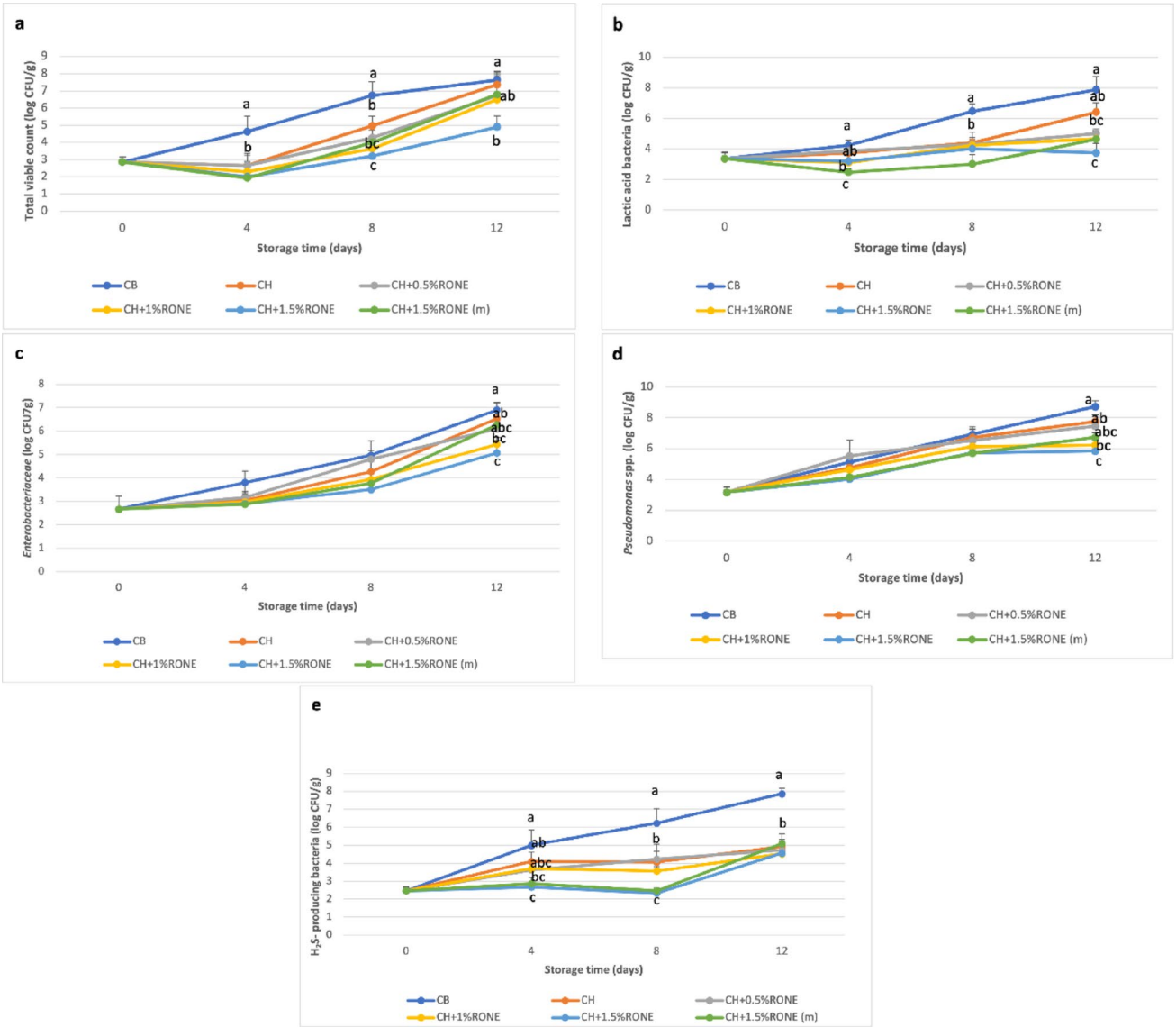


Fig. 5 Microbiological count results of minced beef throughout 12 days storing at 4 °C. **a** Total viable count (TVC); **b** Lactic acid bacteria; **c** *Enterobacteriaceae*; **d** *Pseudomonas* spp.; **e** H_2S-producing bacteria

rates, indicating potential for controlled vanillin release and extended food shelf life [76]. In another study, the controlled release of lysozyme from polyvinyl alcohol films was investigated, demonstrating that the release rate of lysozyme could be controlled, leading to extended antimicrobial activity [77].

LAB, as Gram-positive microorganisms, are resilient to challenging storage conditions such as freezing, low water activity, high salt concentrations, and elevated levels of carbon dioxide. However, they are generally more sensitive to the antimicrobial effects of essential oils compared to Gram-negative bacteria [78]. In this study, the LAB count which was 3.36 log CFU/g on the first day was reduced by CH + 1% RONE, CH + 1.5% RONE, and CH + 1.5% RONE (m) treated groups on day 4, with the highest reduction observed in the CH + 1.5% RONE (m) treated group. The highest values were recorded in the CPB treated group all days. On the 8 th day, the LAB count in the CPB treated group exceeded 6 log CFU/g, while it remained below this value in the other groups. On the 12 th day, the LAB count stayed below 6 log CFU/g in all groups, except for the CPB and CH treated groups. This indicates that the films containing RONE were able to extend the storage time up to 12 days. On day 12, a reduction in LAB count was observed in the CH + 1.5% RONE treated group. The decrease in LAB count on day 4 in the CH + 1.5% RONE (m) treated group suggests a synergistic effect due to the rapid release of 1.5% RONE concentration from the film matrix and chitosan. The decrease observed on day 12 in the CH + 1.5% RONE treated group indicates that RONE's controlled release allows its

antimicrobial effect to persist over a longer period. Similar to our results, Guler et al. [79] demonstrated that quinoa biofilms enriched with essential oils from *Nigella sativa* and *Mentha piperita* significantly reduced LAB counts in rainbow trout fillets, thus extending their shelf life. Kačániová et al. [80] noted that oregano oil at a concentration of 1% significantly decreased LAB populations in chicken thighs, particularly when combined with modified atmosphere packaging. Similarly, Farias et al. [81] assessed the antioxidant and antimicrobial properties of essential oils from various plants, finding that they effectively reduced LAB counts in food matrices.

Compared to the CPB treated group, the growth rate of the *Enterobacteriaceae* population progressed more slowly in the other groups up to day 4. On day 8, *Enterobacteriaceae* in the CPB treated group reached the acceptable upper limit of 5 log CFU/g, while it remained below this level in all other treatment groups, with no statistically significant differences observed among these groups ($p > 0.05$). On day 12, the lowest *Enterobacteriaceae* count (5.06 log CFU/g) was detected in the CH +1.5% RONE treated group, and the growth rate of *Enterobacteriaceae* in this group was found to be lower. The slower growth rate of *Enterobacteriaceae* observed on day 12 in this group can be attributed to the slower release of RONE and its prolonged antibacterial effect. Conversely, on day 12, the Enterobacteriaceae growth rate in the CH +1.5% RONE (m) treated group was nearly as high as in the CPB group (approximately 2.5 log CFU/g). The slower growth rate observed in earlier days in this group may be due to the rapid release of RONE, which exerted its effect for a limited period.

Pseudomonas spp. are known for their psychrotrophic nature, enabling them to grow effectively at refrigeration temperatures [82]. These bacteria are commonly associated with meat spoilage, manifesting as off-odors, discoloration, and gas production, primarily due to their ability to thrive in aerobic conditions [83, 84]. As key spoilage organisms in refrigerated meat, *Pseudomonas* spp. are monitored to maintain meat quality. Acceptable levels are generally considered to be below 3 log CFU/g, as counts exceeding 6 log CFU/g are indicative of advanced spoilage [85].

In the CPB treated group, *Pseudomonas* spp. counts increased from 3.16 log CFU/g on the first day to 8.73 log CFU/g on day 12, indicating significant spoilage. Although the CH and CH +0.5% RONE treated groups exhibited lower counts compared to the CPB treated group. Their *Pseudomonas* spp. levels on day 12 exceeded the spoilage limit, reaching 7.76 and 7.46 log CFU/g, respectively.

In contrast, the CH +1% RONE, CH +1.5% RONE, and CH +1.5% RONE (m) treated groups demonstrated lower *Pseudomonas* spp. counts than CPB and CH treated groups on day 12 ($p < 0.05$). Notably, between days 8 and 12, the growth rate of *Pseudomonas* spp. in the CH +1% RONE and CH +1.5% RONE treated groups was slower. During this same period, the growth rate in the CH +1.5% RONE (m) treated group was higher compared to the CH +1% RONE and CH +1.5% RONE treated groups.

On day 12, *Pseudomonas* spp. counts in the CH +1% RONE, CH +1.5% RONE, and CH +1.5% RONE (m) groups were recorded as 6.23, 5.83, and 6.73 log CFU/g, respectively ($p > 0.05$). These results suggest that these three groups can potentially extend the shelf life to day 12 by maintaining microbial counts below the acceptable spoilage limit.

Similar to the findings of this study, Bayomi et al. [86] evaluated the microbial profile of rabbit meat coated with chitosan and rosemary oil. Their results demonstrated that the treated group showed significantly lower meat demerit scores compared to the untreated group on the 12 th day. They also found that a coating with 1% chitosan and 0. 2% REO effectively reduced the counts of *Enterobacteriaceae*, *Pseudomonas* spp., and psychrotrophic bacteria. Another study demonstrated that chitosan and rosemary extract effectively inhibited the growth of psychrotrophic bacteria in beef [87].

H_2S-producing bacteria in foods cause the degradation of amino acids and proteins. This process leads to off-odors and undesirable flavors, particularly in protein-rich foods like meat [88].

For H_2S-producing bacteria, the initial count of 2.46 log CFU/g increased to 5 log CFU/g by day 4 in the CPB treated group. On the same day, the counts were 2.88 log CFU/g in the CH +1.5% RONE group and 2.46 log CFU/g in the CH +1.5% RONE (m) treated group ($p > 0.05$). In the CH +1% RONE and CH +0.5% RONE treated groups, the counts rose to 3.56 and 4.23 log CFU/g, respectively. The CH +1.5% RONE and CH +1.5% RONE (m) treated groups exhibited slower growth, likely due to the higher concentration of antimicrobial RONE.

By day 8, growth rates in CH +1.5% RONE, CH +1.5% RONE (m), and CH +1% RONE treated groups had decreased. This could be attributed to the sustained release of the nanoemulsion. However, on day 12, the H_2S-producing bacteria counts in the CH +1.5% RONE and CH +1.5% RONE (m) treated groups were found to be similar ($p < 0.05$), possibly due to the gradual decrease in antimicrobial activity over time or the metabolic characteristics and adaptability of H_2S-producing bacteria might have contributed to this result. Studies have reported that essential oil-enriched films possess inhibitory effects on H2S-producing bacteria.

Similar to our findings, studies have demonstrated that chitosan films containing essential oils can effectively

reduce the growth of H_2S-producing bacteria, thereby improving meat quality and safety [89, 90].

Conclusion

In this study, three-layer chitosan films enriched with RONE were suggested to have the potential to extend the shelf life of minced beef compared to commercial plastic bags and monolayer films incorporated with RONE. These films demonstrated an ability to delay microbial growth and lipid oxidation while maintaining protein quality, as indicated by a reduction in TVN values. The three-layer films containing 1.5% RONE appeared to be particularly effective in suppressing spoilage microorganisms such as Pseudomonas spp. and H_2S-producing bacteria after day 4. However, by the final day of storage (day 12), no statistically significant differences were observed between the three-layer and monolayer films in terms of microbial counts. Despite the incorporation of RONE, no significant changes were observed in the mechanical properties of the films, such as TS and EAB.

This study highlights the potential of multilayer chitosan films as a sustainable alternative to traditional food packaging. However, some improvements are needed. The slight reduction in hydrophobicity observed in RONE-containing films may affect moisture resistance, suggesting that optimization of nanoemulsion formulations and strengthening of film structural properties could be beneficial. Additionally, sensory evaluations and consumer acceptance studies would be valuable to ensure the practical usability of these films in real-world applications.

Future research may consider the integration of additional natural bioactive compounds to enhance antimicrobial efficacy against a broader range of microorganisms. Assessing the long-term stability of the films under various storage conditions could provide valuable insights for broader applications. Additionally, further studies are needed to evaluate the applicability of these findings to different food products.

Acknowledgements This study was funded by Kafkas University Scientific Research Projects Coordination Unit (Grant Number: 2023-FM-62). The authors would like to express their gratitude for the financial support provided.

Author contributions N.M.: Investigation, Resources, Data Curation, Visualization, Writing – Original Draft, Writing – Review & Editing. B.M.: Conceptualization, Methodology, Formal Analysis, Project Administration, Supervision.

Funding Open access funding provided by the Scientific and Technological Research Council of Türkiye (TÜBİTAK).
This study was funded by Kafkas University Scientific Research Projects Coordination Unit (Grant Number: 2023-FM-62).

Data availability No datasets were generated or analysed during the current study.

Declarations

Conflict of interest The authors declare no competing interests.

Open Access This article is licensed under a Creative Commons Attribution 4.0 International License, which permits use, sharing, adaptation, distribution and reproduction in any medium or format, as long as you give appropriate credit to the original author(s) and the source, provide a link to the Creative Commons licence, and indicate if changes were made. The images or other third party material in this article are included in the article's Creative Commons licence, unless indicated otherwise in a credit line to the material. If material is not included in the article's Creative Commons licence and your intended use is not permitted by statutory regulation or exceeds the permitted use, you will need to obtain permission directly from the copyright holder. To view a copy of this licence, visit http://creativecommons.org/licenses/by/4.0/.

References

1. Park JM, Lee AR, Hong JW, Ghim S (2019) Microbial risks in food franchise: a step forward in establishing ideal cleaning and disinfection practices in SOPPs. J Food Saf 39:e12606. https://doi.org/10.1111/jfs.12606
2. Malavi D, Muzhingi T, Abong GO (2018) Good manufacturing practices and microbial contamination sources in orange fleshed sweet potato puree processing plant in Kenya. Int J Food Sci 2018:4093161. https://doi.org/10.1155/2018/4093161
3. Zhang X, Guo M, Ismail BB, He Q, Jin T, Liu D (2021) Informative and corrective responsive packaging: advances in farm-to-fork monitoring and remediation of food quality and safety. Compr Rev Food Sci Food Saf 20:5258–5282. https://doi.org/10.1111/1541-4337.12807
4. Leong CR, Daud NS, Tong WY, Cheng SY, Tan WN, Hamin NS, Pa'ee KF (2021) Gelatine film incorporated with Clitoria ternatea-derived anthocyanin microcapsules, a food packaging material effective against foodborne pathogens. Food Technol Biotechnol 59:422–431. https://doi.org/10.17113/ftb.59.04.21.7069
5. Karanth S, Feng S, Patra D, Pradhan AK (2023) Linking microbial contamination to food spoilage and food waste: the role of smart packaging, spoilage risk assessments, and date labeling. Front Microbiol 14:1198124. https://doi.org/10.3389/fmicb.2023.1198124
6. Aloui H, Khwaldia K (2016) Natural antimicrobial edible coatings for microbial safety and food quality enhancement. Compr Rev Food Sci Food Saf 15:1080–1103. https://doi.org/10.1111/1541-4337.12226
7. Prüβ BM (2020) Microbes in our food, an ongoing problem with new solutions. Antibiotics 9:584. https://doi.org/10.3390/antibiotics9090584
8. Gao Q, Feng Z, Wang J, Zhao F, Li C, Ju J (2024) Application of nano-ZnO in the food preservation industry: antibacterial mechanisms, influencing factors, intelligent packaging, preservation film and safety. Crit Rev Food Sci Nutr. 2024:1–27. https://doi.org/10.1080/10408398.2024.2387327
9. Feng Z, Sun P, Zhao F, Li M, Ju J (2024) Advancements and challenges in biomimetic materials for food preservation: A review. Food Chem 2024:141119. https://doi.org/10.1016/j.foodchem.2024.141119

10. Wang J, Gao Q, Zhao F, Ju J (2023) Repair mechanism and application of self-healing materials for food preservation. Crit Rev Food Sci Nutr 64:11113–11123. https://doi.org/10.1080/10408398.2023.2232877
11. Gao Q, Qi J, Tan Y, Ju J (2024) Antifungal mechanism of Angelica sinensis essential oil against penicillium roqueforti and its application in extending the shelf life of bread. Int J Food Microbiol 408:110427. https://doi.org/10.1016/j.ijfoodmicro.2023.110427
12. Feng Z, Zhang Q, Wang Y, Yang Q, Li C, Zhao F, Ju J (2025) Anti-Aspergillus Niger mechanism of small molecular combinations of essential oils and their application in extending the shelf-life of bread. Food Biosci 64:105979. https://doi.org/10.1016/j.fbio.2025.105979
13. Ju J, Xie Y, Yu H, Guo Y, Cheng Y, Zhang R, Yao W (2020) Synergistic Inhibition effect of Citral and Eugenol against Aspergillus Niger and their application in bread preservation. Food Chem 310:125974. https://doi.org/10.1016/j.foodchem.2019.125974
14. Yang P, Huo Y, Yang Q, Zhao F, Li C, Ju J (2025) Synergistic anti-biofilm strategy based on essential oils and its application in the food industry. World J Microbiol Biotechnol 41:1–22. https://doi.org/10.1007/s11274-025-04289-8
15. Ju J, Xie Y, Guo Y, Cheng Y, Qian H, Yao W (2019) Application of edible coating with essential oil in food preservation. Crit Rev Food Sci Nutr 59:2467–2480. https://doi.org/10.1080/10408398.2018.1456402
16. Amjadi S, Almasi H, Ghadertaj A, Mehryar L (2021) Whey protein isolate-based films incorporated with nanoemulsions of orange Peel (Citrus sinensis) essential oil: Preparation and characterization. J Food Process Preserv 45:e15196. https://doi.org/10.1111/jfpp.15196
17. Liu X, Jia J, Duan S, Zhou X, Xiang A, Lian Z, Ge F (2020) Zein/mcm-41 nanocomposite film incorporated with cinnamon essential oil loaded by modified supercritical CO2 impregnation for long-term antibacterial packaging. Pharmaceutics 12:169. https://doi.org/10.3390/pharmaceutics12020169
18. Yang H, Wang J, Yang F, Chen M, Zhou D, Li L (2016) Active packaging films from ethylene vinyl alcohol copolymer and clove essential oil as shelf life extenders for grass carp slice. Packag Technol Sci 29:383–396. https://doi.org/10.1002/pts.2215
19. Zhang W, Shu C, Chen Q, Cao J (2019) The multi-layer film system improved the release and retention properties of cinnamon essential oil and its application as coating in Inhibition to penicillium expansion of Apple fruit. Food Chem 299:125109. https://doi.org/10.1016/j.foodchem.2019.125109
20. Zhu B, Liu Y, Qin Y, Chen H, Zhou L (2021) Release of clove essential oil loaded by mesoporous nano-silica in polylactic acid-based food packaging on postharvest preservation of white button mushroom. Int J Food Sci Technol 57:457–465. https://doi.org/10.1111/ijfs.15440
21. Mondal MIH (2021) Recent advancement of PVA/chitosan-based composite biofilm for food packaging. Biomed J Sci Tech Res 46:36982–36986. https://doi.org/10.26717/bjstr.2022.46.007286
22. Lan W, Du J, Wang M, Xie J (2022) Effects of Chitosan coating on quality and protein characteristics of large yellow croaker (Pseudosciaena crocea) during ice storage. J Food Process Preserv 46:e16649. https://doi.org/10.1111/jfpp.16649
23. Orgaz B, Lobete MM, Puga CH, José CS (2011) Effectiveness of Chitosan against mature biofilms formed by food related bacteria. Int J Mol Sci 12:817–828. https://doi.org/10.3390/ijms12010817
24. Amankwaah C, Lǐ J, Lee J, Pascall MA (2020) Antimicrobial activity of chitosan-based films enriched with green tea extracts on murine Norovirus, Escherichia coli, and Listeria innocua. Int J Food Sci 2020:1–9. https://doi.org/10.1155/2020/3941924
25. Nair SB, Alummoottil NJ, Moothandasserry SS (2017) Chitosan-konjac glucomannan-cassava starch-nanosilver composite films with moisture resistant and antimicrobial properties for food-packaging applications. Starch-Stärke 69:1600210. https://doi.org/10.1002/star.201600210
26. Wang S, Jing Y (2016) Effects of a Chitosan coating layer on the surface properties and barrier properties of kraft paper. BioResources 11:1868–1881. https://doi.org/10.15376/biores.11.1.1868-1881
27. Abdollahi M, Rezaei M, Farzi G (2012) Improvement of active Chitosan film properties with Rosemary essential oil for food packaging. Int J Food Sci Technol 47:847–853. https://doi.org/10.1111/j.1365-2621.2011.02917.x
28. Mutlu N (2023) Effects of grape seed oil nanoemulsion on physicochemical and antibacterial properties of gelatin sodium alginate film blends. Int J Bio Macromol 237:124207. https://doi.org/10.1016/j.ijbiomac.2023.124207
29. ASTM (2016) Standard test methods for water vapor transmission of materials. In Annual book of ASTM standards, pp. 719–725. American Society for Testing and Materials. https://doi.org/10.1520/E0096_E0096M-16
30. Setyabrata D, Kim YH (2019) Impacts of aging/freezing sequence on microstructure, protein degradation and physico-chemical properties of beef muscles. Meat Sci 151:64–74. https://doi.org/10.1016/j.meatsci.2019.01.007
31. Ye L, Wang H, Duncan SE, Eigel WN, O'Keefe SF (2015) Antioxidant activities of vine tea (Ampelopsis grossedentata) extract and its major component Dihydromyricetin in soybean oil and cooked ground beef. Food Chem 172:416–422. https://doi.org/10.1016/j.foodchem.2014.09.090
32. Mohammadi H, Kamkar A, Misaghi A, Žunabović-Pichler M, Fatehi S (2019) Nanocomposite films with CMC, Okra mucilage, and ZnO nanoparticles: extending the shelf-life of chicken breast meat. Food Packag Shelf Life 21:100330. https://doi.org/10.1016/j.fpsl.2019.100330
33. Angioni A, Barra A, Cereti E, Barile D, Coïsson JD, Arlorio M, Cabras P (2004) Chemical composition, plant genetic differences, antimicrobial and antifungal activity investigation of the essential oil of Rosmarinus officinalis L. J Agric Food Chem 52:3530–3535. https://doi.org/10.1021/jf049913t
34. Pintore GAM, Usaï M, Bradesi P, Juliano CCA, Boatto G, Tomi F, Casanova J (2001) Chemical composition and antimicrobial activity of Rosmarinus officinalis L. oils from Sardinia and Corsica. Flavour Fragr J 17:15–19. https://doi.org/10.1002/ffj.1022
35. El-Kelany A (2020) Phytochemical and biological studies on some medicinal plants. Al-Azhar J Pharm Sci 62:110–134. https://doi.org/10.21608/ajps.2020.118379
36. Sadia B (2016) Chemical composition of Rosemary (Rosmarinus officinalis L.) leaves under salt stress. Pure Appl Biol 5:355–360. https://doi.org/10.19045/bspab.2016.50046
37. Hussain AI, Anwar F, Chatha SAS, Jabbar A, Mahboob S, Nigam PSN (2010) Rosmarinus officinalis essential oil: antiproliferative, antioxidant and antibacterial activities. Braz J Microbiol 41:1070–1078. https://doi.org/10.1590/s1517-83822010000400027
38. Sharma P, Pant S, Rai S, Yadav R, Sharma S, Dave V (2017) Green synthesis and characterization of silver nanoparticles by Allium cepa L. to produce silver nano-coated fabric and their antimicrobial evaluation. Appl Organomet Chem 32:e4146. https://doi.org/10.1002/aoc.4146
39. Hanasaki M, Nagata F, Miyajima T, Kato K (2018) Controlling particle size of poly(lactic acid)/hydroxyapatite nanoparticles. Trans Mat Res Soc Japan 43:135–138. https://doi.org/10.14723/tmrsj.43.135
40. Woehl T, Park C, Evans J, Arslan I, Ristenpart W, Browning N (2014) Direct observation of aggregative nanoparticle growth: kinetic modeling of the size distribution and growth rate. Microsc

Microanal 20:1612–1613. https://doi.org/10.1017/s1431927614009799
41. Liu W, Yang A, Li Z, Xu H, Yang X (2007) PEGylated PLGA nanoparticles as tumor necrosis factor-α receptor blocking peptide carriers: preparation, characterization and release in vitro. J Wuhan Univ Technol Mater 22:112–116. https://doi.org/10.1007/s11595-005-1112-4
42. Kalidas S, Geetha P (2022) Development and optimization of astragalin-loaded polymeric nanoparticles using central composite factorial design. Int J Appl Pharm 14:69–77. https://doi.org/10.22159/ijap.2022v14i5.44315
43. Hu X, Shi C, Yuan Q, Zhang J, De Schutter G (2018) Influences of chloride immersion on zeta potential and chloride concentration index of cement-based materials. Cem Concr Res 106:49–56. https://doi.org/10.1016/j.cemconres.2018.01.015
44. Yu H, Zhang C, Xie Y, Mei J, Xie J (2022) Effect of Melissa officinalis L. essential oil nanoemulsions on structure and properties of carboxymethyl Chitosan/locust bean gum composite films. Membranes 12:568. https://doi.org/10.3390/membranes12060568
45. Jantrawut P, Boonsermsukcharoen K, Thipnan K, Chaiwarit T, Hwang K, Park ES (2018) Enhancement of antibacterial activity of orange oil in pectin thin film by microemulsion. Nanomaterials 8:545. https://doi.org/10.3390/nano8070545
46. Honary S, Zahir F (2013) Effect of zeta potential on the properties of nano-drug delivery systems—a review (part 2). Trop J Pharm Res 12:265–273. https://doi.org/10.4314/tjpr.v12i2.20
47. Guerra-Rosas MI, Morales-Castro J, Ochoa-Martínez LA, Salvia-Trujillo L, Martín-Belloso O (2016) Long-term stability of food-grade nanoemulsions from high methoxyl pectin containing essential oils. Food Hydrocoll 52:438–446. https://doi.org/10.1016/j.foodhyd.2015.07.017
48. Otoni CG, Pontes SFO, Medeiros EAA, Soares NFF (2014) Edible films from Methylcellulose and nanoemulsions of clove bud (Syzygium aromaticum) and oregano (Origanum vulgare) essential oils as shelf life extenders for sliced bread. J Agric Food Chem 62:5214–5219. https://doi.org/10.1021/jf501055f
49. Ziani K, Chang Y, McLandsborough L, McClements DJ (2011) Influence of surfactant charge on antimicrobial efficacy of surfactant-stabilized thyme oil nanoemulsions. J Agric Food Chem 59:6247–6255. https://doi.org/10.1021/jf200450m
50. Frank K, Garcia C, Shin G, Kim J (2018) Alginate biocomposite films incorporated with cinnamon essential oil nanoemulsions: physical, mechanical, and antibacterial properties. Int J Polym Sci 2018:1519407. https://doi.org/10.1155/2018/1519407
51. Taqi A, Mutihac L, Stamatin I (2013) Physical and barrier properties of Apple Pectin/cassava starch composite films incorporating Laurus nobilis L. oil and oleic acid. J Food Process Preserv 38:1982–1993. https://doi.org/10.1111/jfpp.12174
52. Cerqueira M, Souza B, Teixeira J (2012) Effect of glycerol and corn oil on physicochemical properties of polysaccharide films – a comparative study. Food Hydrocoll 27:175–184. https://doi.org/10.1016/j.foodhyd.2011.07.007
53. Restrepo A, Rojas J, García O, Sánchez L, Pinzón M, Villa C (2018) Mechanical, barrier, and color properties of banana starch edible films incorporated with nanoemulsions of Lemongrass (Cymbopogon citratus) and Rosemary (Rosmarinus officinalis) essential oils. Food Sci Technol Int 24:705–712. https://doi.org/10.1177/1082013218792133
54. Souza V, Monte M, Pinto L (2011) Preparation of biopolymer film from Chitosan modified with lipid fraction. Int J Food Sci 46:1856–1862. https://doi.org/10.1111/j.1365-2621.2011.02692.x
55. Lu W, Huang D, Wang C, Yeh C, Tsai J, Huang Y, Li P (2018) Preparation, characterization, and antimicrobial activity of nanoemulsions incorporating Citral essential oil. J Food Drug Anal 26:82–89. https://doi.org/10.1016/j.jfda.2016.12.018
56. Wang K, Hong Y, Gu Z, Cheng L, Li Z, Li C (2022) Fabrication and characterisation of spice essential oil-based nanoemulsions: physical, sensory and antimicrobial properties. Int J Food Sci Technol 57:7852–7861. https://doi.org/10.1111/ijfs.16131
57. Hasssanzadeh H, Alizadeh M, Bari M (2018) Formulation of Garlic oil-in-water nanoemulsion: antimicrobial and physicochemical aspects. IET Nanobiotechnol 12:647–652. https://doi.org/10.1049/iet-nbt.2017.0104
58. Marchi M, Righi F, Meneghesso M, Manfrin D, Ricci R (2016) Prediction of chemical composition and peroxide value in unground pet foods by near-infrared spectroscopy. J Anim Physiol Anim Nutr 102:337–342. https://doi.org/10.1111/jpn.12663
59. Abeyrathne E, Nam K, Ahn D (2021) Analytical methods for lipid oxidation and antioxidant capacity in food systems. Antioxidants 10:1587. https://doi.org/10.3390/antiox10101587
60. Francis A (2019) Variety of watermelon and method of drying affect the chemical and functional characteristics of oils extracted from watermelon seeds. Res J Food Nutr 3:17–24. https://doi.org/10.22259/2637-5583.0302004
61. Adelagun R, Berezi EP, Fagbemi JO, Igbaro OJ, Aihkoje FE, Ngana O, Garba MS (2023) Evaluation of level of rancidity of edible oil in some fried snacks food. JCNS 48:154–161. https://doi.org/10.46602/jcsn.v48i1.853
62. Liao S, Tian L, Qi Q, Hu L, Wang M, Gao C, Gong G (2023) Transcriptome analysis of Protocatechualdehyde against listeria monocytogenes and its effect on chicken quality characteristics. Foods 12:2625. https://doi.org/10.3390/foods12132625
63. Menon V, Ram M, Dorn JM, Armstrong D, Muti P, Freudenheim JL, Trevisan M (2004) Oxidative stress and glucose levels in a population-based sample. Diabet Med 21:1346–1352. https://doi.org/10.1111/j.1464-5491.2004.01417.x
64. Gómez FS, Pablos MPA (2016) Pineapple waste extract for preventing oxidation in model food systems. J Food Sci 81:C1622–C1628. https://doi.org/10.1111/1750-3841.13341
65. Choe J, Kim H, Kim C (2017) Effect of persimmon Peel (Diospyros Kaki Thumb.) extracts on lipid and protein oxidation of Raw ground pork during refrigerated storage. Korean J Food Sci an 37:254–263. https://doi.org/10.5851/kosfa.2017.37.2.254
66. Hęś M, Szwengiel A, Dziedzic K, Thanh-Blicharz JL, Kmiecik D, Górecka D (2017) The effect of buckwheat hull extract on lipid oxidation in frozen-stored meat products. J Food Sci 82:882–889. https://doi.org/10.1111/1750-3841.13682
67. Yu D, Xu Y, Jiang Q, Xia W (2017) Effects of Chitosan coating combined with essential oils on quality and antioxidant enzyme activities of grass carp (Ctenopharyngodon idellus) fillets stored at 4°C. Int J Food Sci Technol 52:404–412. https://doi.org/10.1111/ijfs.13295
68. Christopoulou SD, Androutsopoulou C, Hahalis P, Kotsalou C, Vantarakis A, Lamari FN (2021) Rosemary extract and essential oil as drink ingredients: an evaluation of their chemical composition, genotoxicity, antimicrobial, antiviral, and antioxidant properties. Foods 10:3143. https://doi.org/10.3390/foods10123143
69. Choi S, Jang G, Choi S, Jung T, Cho B, Sim W et al (2019) Development and validation of an analytical method for carnosol, carnosic acid and Rosmarinic acid in food matrices and evaluation of the antioxidant activity of Rosemary extract as a food additive. Antioxidants 8:76. https://doi.org/10.3390/antiox8030076
70. Javanmard M (2020) Effects of grape and pomegranate waste extracts on poultry carcasses microbial, chemical, and sensory attributes in slaughterhouse. Food Sci Nutr 8:5622–5630. https://doi.org/10.1002/fsn3.1840
71. Oraei M, Motallebi A, Hoseini E, Javan S (2012) Effect of gamma irradiation and frozen storage on chemical and sensory

characteristics of rainbow trout (Oncorhynchus mykiss) fillet. Int J Food Sci Technol 47:977–984. https://doi.org/10.1111/j.1365-2621.2011.02930.x
72. Elsaka SE, Elnaghy AM (2012) Effect of addition of Chitosan to self-etching primer: antibacterial activity and push-out bond strength to radicular dentin. J Biomed Res 26:288. https://doi.org/10.7555/jbr.26.20120042
73. Munteanu BS, Săcărescu L, Vasiliu A, Hitruc G, Pricope GM, Sivertsvik M et al (2018) Antioxidant/antibacterial electrospun nanocoatings applied onto PLA films. Materials 11:1973. https://doi.org/10.3390/ma11101973
74. Hellali DH, Ayachi N (2023) Nanoencapsulation of Rosmarinus officinalis essential oil into Chitosan crosslinked to tripolyphosphate nanoparticles and alginate/chitosan nanoparticles: formulation, characterization, in vitro release study, and in vivo evaluation. J Drug Deliv Ther 13:45–55. https://doi.org/10.22270/jddt.v13i11.6270
75. Farokhzad P, Dastgerdi AA, Nimavard JT (2023) The effect of Chitosan and Rosemary essential oil on the quality characteristics of chicken burgers during storage. J Food Process Preserv 2023:8381828. https://doi.org/10.1155/2023/8381828
76. Stroescu M, Stoica-Guzun A, Jipa IM (2013) Vanillin release from Poly (vinyl alcohol)-bacterial cellulose mono and multilayer films. J Food Eng 114:153–157. https://doi.org/10.1016/j.jfoodeng.2012.08.023
77. Buonocore GG, Conte A, Corbo MR, Sinigaglia M, Del Nobile MA (2005) Mono-and multilayer active films containing lysozyme as antimicrobial agent. Innov Food Sci Emerg Technol 6:459–464. https://doi.org/10.1016/j.ifset.2005.05.006
78. Carrión-Granda X, Fernández-Pan I, Rovira J, Maté J (2018) Effect of antimicrobial edible coatings and modified atmosphere packaging on the Microbiological quality of cold stored Hake (Merluccius merluccius) fillets. J Food Qual 2018:6194906. https://doi.org/10.1155/2018/6194906
79. Guler K, Yanık T, Alak G (2022) Investigations on the shelf life of rainbow trout fillets covered by Quinoa biofilms enriched with different essential oils (Nigella sativa and Mentha piperita). Food Sci Technol Int 30:251–259. https://doi.org/10.1177/10820132221145973
80. Kačániová M, Mellen M, Vukovic NL, Kluz M, Puchalski C, Haščík P, Kunová S (2019) Combined effect of vacuum packaging, fennel and savory essential oil treatment on the quality of chicken thighs. Microorganisms 7:134. https://doi.org/10.3390/microorganisms7050134
81. Farias PKS, Silva JCRL, Souza NCD, Fonseca FSAD, Brandi IV, Martins ER et al (2019) Antioxidant activity of essential oils from condiment plants and their effect on lactic cultures and pathogenic bacteria. Ciência Rural 49:e20180140. https://doi.org/10.1590/0103-8478cr20180140
82. Dourou D, Spyrelli E, Doulgeraki A, Argyri A, Grounta A, Nychas G et al (2021) Microbiota of chicken breast and thigh fillets stored under different refrigeration temperatures assessed by next-generation sequencing. Foods 10:765. https://doi.org/10.3390/foods10040765
83. Wickramasinghe N, Ravensdale J, Coorey R, Chandry S, Dykes G (2019) The predominance of psychrotrophic pseudomonads on aerobically stored chilled red meat. Compr Rev Food Sci Food Saf 18:1622–1635. https://doi.org/10.1111/1541-4337.12483
84. Watson S, Furbeck R, Fernando S, Chaves B, Sullivan G (2023) Spoilage pseudomonas survive common thermal processing schedules and grow in emulsified meat during extended vacuum storage. J Food Sci 88:2162–2167. https://doi.org/10.1111/1750-3841.16557
85. Zawani CJ, Nor-Khaizura MAR, Mahyudin NA, Ismail-Fitry MR, Nirmal NP (2022) Microbiological and sensorial quality of beef meat (Longissimus dorsi) marinated with cinnamon extract and stored at various temperatures. Foods 11:3971. https://doi.org/10.3390/foods11243971
86. Bayomi RME, Shata RHM, Mahmoud AFA (2023) Effects of edible Chitosan coating containing salvia Rosmarinus essential oil on quality characteristics and shelf life extension of rabbit meat during chilled storage. J Food Meas Charact 17:2464–2474. https://doi.org/10.1007/s11694-023-01804-z
87. de Lima AF, Leite RHDL, Pereira MWF, Silva MRL, de Araújo TLAC, de Lima Júnior DM et al (2024) Chitosan coating with Rosemary extract increases shelf life and reduces water losses from beef. Foods 13:1353. https://doi.org/10.3390/foods13091353
88. Kushkevych I, Đorđević Đ, Kollár P, Vítězová M, Drago L (2019) Hydrogen sulfide as a toxic product in the small–large intestine axis and its role in IBD development. J Clin Med 8:1054. https://doi.org/10.3390/jcm8071054
89. Hernández H, Fraňková A, Sýkora T, Klouček P, Kouřimská L, Kucerova I, Banout J (2016) The effect of oregano essential oil on microbial load and sensory attributes of dried meat. J Sci Food Agric 97:82–87. https://doi.org/10.1002/jsfa.7685
90. Al-Hijazeen M, Lee E, Mendonça A, Ahn D (2016) Effect of oregano essential oil (Origanum vulgare subsp. hirtum) on the storage stability and quality parameters of ground chicken breast meat. Antioxidants 5:18. https://doi.org/10.3390/antiox5020018

Publisher's note Springer Nature remains neutral with regard to jurisdictional claims in published maps and institutional affiliations.